IRANIAN JOURNAL OF CATALYSIS

Synthesis of Ag-Ag_2O nanoparticles using *Ageratum conyzoides* leaf extract for the catalytic reduction of nitrobenzene and methylene blue and antibacterial applications

Dinesh Mahadev Patil[a], Kagepura Thammaiah Chandrashekara[b], Jayappa Manjanna[a,*], Malavalli Basavaraju Sridhara [a,*]

a) Department of Chemistry, Rani Channamma University, Belagavi 591 156, Karnataka, India
b) Institute of Excellence, Vijnana Bhavana, University of Mysore, Mysuru 570 006, Karnataka, India

Received 7 November 2022; received in revised form 8 January 2023; accepted 5 February 2023 **(DOI: 10.30495/IJC.2023.1972239.1972)**

ABSTRACT

The 4-nitrophenol (4-NP) and methylene blue (MB) are commonly used in many industries and remain in the industrial effluent. They have an adverse effect on the environment if not treated properly. Therefore, it is essential to develop a convenient method to remove such toxic chemicals from wastewater. Here, Ag/Ag_2O nanoparticles (NPs) were prepared from $AgNO_3$ (0.05 M) using *Ageratum conyzoides L*. agricultural weed extract (50 mL) in an ultrasonic bath. Then, the synthesized Ag/Ag_2O NPs were utilized for the 4-NP and MB reduction in the presence of $NaBH_4$. The Ag/Ag_2O NPs efficiently reduce 4-NP to 4-AP and MB to LMB in an aqueous medium. In the case of 4-NP, about 93% of the reduction was achieved in about 10 min at optimum conditions, 2 mL of 4-NP (0.15 mM) and 100 µL of $NaBH_4$ (50 mM) in the presence of 1 mg Ag/Ag_2O NPs. About 94% reduction of MB dye was achieved in about 6 min at optimum conditions, 2 mL of MB (10 ppm) and 100 µL of $NaBH_4$ (30 mM) using 1 mg Ag/Ag_2O NPs. Furthermore, the bactericidal activity of Ag/Ag_2O NPs was studied against *S. Mutans, B. Subtilis,* and *E. coli.*

Keywords*: Ageratum conyzoides; Ag/Ag_2O; Antibacterial activity; Methylene blue; 4-nitrophenol.*

1. Introduction

Most industries such as pesticides, dyes, explosives, rubber, pharmaceutical, paint, etc., utilize nitroaromatic compounds as a precursor in the synthesis of end products [1-4]. Although nitroaromatic compounds are industrially important chemicals, their toxic and carcinogenic nature affects the environment and animals, if discharged untreated [1, 3, 5]. Therefore, several studies have reported removing highly toxic nitroaromatic compounds by reducing the nitro-group to a less toxic amino-group [6-10]. There are several organic and inorganic pollutants in the environment which cause severe soil, air, and water pollution. The organic pollutants include lindane, hexachlorocyclohexane, chlorpyrifos, biphenyl, 4-chlorobiphenyl, phenanthrene, pyrene, metronidazole, reactive blue 255, and fenitrothion. On the other hand, inorganic pollutants comprise highly toxic non-biodegradable heavy metals such as Hg, Cd, Zn, Pb, Ni, Cr, As, Se, Sb, Cs, Sr, Pu, and Am [11-16]. Methylene blue is a heterocyclic aromatic compound commonly utilized by the textile and dye industry. In 2022, the textile dyes market is $11 billion and is estimated to grow to $14 billion by 2027 with a 4.6% CAGR. The dyes market is growing as its demand in various industries such as textiles, paints, coatings, construction, and plastics increased [17]. Textile dyeing utilizes large amounts of water. It was calculated that about 100 to 150 L of water is consumed to process 1000 gm of textile [18]. Besides industrial applications, MB is used in medication and in chemistry as a redox indicator. It also acts as an antimalarial agent and peroxide generator. However, upon consumption, it causes nausea, vomiting, diarrhoea, and difficulties in breathing [19].

*Corresponding author:
E-mail address: sridhara.mb@gmail.com (**M. B. Sridhara**); jmanjanna@rediffmail.com (**J. Manjanna**)

The metal/metal oxide NPs have attracted researchers due to their applications in various fields such as photocatalysis, bio-sensors, chemical sensors, bactericidal, antioxidant, etc. [20-26]. Ag is a very interesting metal showing promising catalytic and antimicrobial activity. Chandraker et al., [20] have studied the synthesis of Ag and its application in DNA-binding, antioxidant, and H_2O_2 sensing. Maham et al., [21] have reported the synthesis of Ag/ZrO_2 nanocomposites to treat environmental pollutants. Ag_2O is a p-type semiconductor with a narrow band gap (~1.3 eV); it is found to be a self-stable and efficient visible-light photocatalyst [27-29]. The Ag NPs are easily oxidized to Ag_2O followed by gradual oxidation to AgO. Therefore, the core-shell structured Ag/Ag_2O (i.e., surface oxidation of $Ag \rightarrow Ag_2O$) is expected to be a relatively stable nanomaterial for real system applications.

Ageratum conyzoides L. is an herbaceous plant which belongs to the Asteraceae family. It is a fast-growing tropical weed, which is commonly found in West Africa, Asia, and South America [30]. Numbers of reports are available on the extraction of chemical compounds such as sesquiterpenes, chromene, chromone, benzofuran, coumarin, flavonoids, triterpene, sterols, alkaloids, saponins, and oxygen heterocycles [20, 21, 30]. The *Ageratum conyzoides L.* plant possesses broad pharmacological properties such as wound healing, anti-inflammatory, antijuvenile hormonal activity, antioxidant, antiviral, skin infection, antifungal, and insecticidal activities [20,21,30,31].

In this context, the ultrasonic-assisted synthesis of Ag/Ag_2O NPs was reported using *Ageratum conyzoides L.* extract at room temperature. *Ageratum conyzoides L.* extract was prepared using a microwave oven in distilled water. The aqueous leaf extract was used to prepare Ag/Ag_2O NPs. Then, the prepared NPs were studied for their catalytic activity in 4-nitrophenol (4-NP) and methylene blue (MB) reduction using $NaBH_4$. Furthermore, the bactericidal activity of Ag/Ag_2O NPs was studied against *S. Mutans, B. Subtilis,* and *E. Coli.*

2. Experimental

The chemicals silver nitrate ($AgNO_3$), 4-NP, sodium borohydride ($NaBH_4$), and MB were of analytical grade. The leaves of *Ageratum conyzoides* weed were collected from the local sugarcane field. A microwave oven was used for the preparation of plant extract. In all the experiments, distilled water was used to prepare the solutions.

2.1 Preparation of plant extract

Fresh leaves of *Ageratum conyzoides* were taken, cleaned, and washed thoroughly with plenty of water. The aqueous leaf extract was prepared by weighing finely cut 20 g of leaves in 200 mL distilled water and kept for microwave irradiation for about (power: 700 W) 5 min. Then, the extract was filtered through membrane filter paper and used for NPs synthesis.

2.2 Synthesis of Ag/Ag_2O NPs

The Ag/Ag_2O NPs were prepared using $AgNO_3$ and an aqueous leaf extract of *Ageratum conyzoides*. Approximately, 2.1 g of $AgNO_3$ was dissolved in 250 mL distilled water (0.05 M) and kept in an ultrasonic bath. To this, 50 mL of plant extract was added dropwise at room temperature (RT), and simultaneous UV-Visible spectra of the reaction mixture were recorded. The color of the reaction mixture changes from reddish-brown to black. Then, the black powder was obtained by filtration with distilled water followed by vacuum drying at RT (25-28 ^{0}C). The black powder was characterized by UV Visible spectroscopy, FT-IR, XRD, and FESEM–EDX. The efficiency of this process is about 66%, which may be less than chemical processes. However, using *ageratum conzoides* to synthesize Ag/Ag_2O reduces the cost of the process as it is an agricultural weed.

2.3 Reduction of 4-nitrophenol

The 4-NP reduction was performed using sodium borohydride in the presence of Ag/Ag_2O NPs at RT (25-28 ^{0}C). In a typical case, 2 mL of 4-NP (0.15 mM) aqueous solution and 100 µL of $NaBH_4$ (50 mM) aqueous solution were placed in a 4 mL quartz cuvette. Then, 1 mg of Ag/Ag_2O NPs was added to the above mixture, and the cuvette was placed in a UV-Visible spectrophotometer, the progress of the reaction was monitored at different time intervals [8, 32].

2.4 Reduction of methylene blue dye

The reduction of MB dye was studied using Ag/Ag_2O NPs in the presence of $NaBH_4$ at RT (25-28 ^{0}C). In a typical case, 2 mL of MB (10 ppm) aqueous solution and 100 µL of $NaBH_4$ (30 mM) aqueous solution were placed in a 4 mL quartz cuvette. Then, 1 mg of Ag/Ag_2O NPs was added to the above mixture, and the cuvette was placed in a UV-Visible spectrophotometer, the progress of the reaction was monitored at different time intervals [19, 33, 34].

2.5 Antibacterial activity

The antimicrobial activity of the above sample was investigated using the well diffusion method. Invitro antibacterial activity of Ag/Ag_2O NPs was investigated using the well (ϕ 6 mm) diffusion method. Test plates were prepared with 20 mL of LB agar. Then 50 µL of sample solution (prepared by dissolving 10 mg and 5 mg of Ag/Ag_2O NPs in 1 mL of DMSO) were added to the well. The wells loaded with sterile media were considered as blank, and 30 µg/40 µL streptomycins as a commercial standard. Plates were incubated at 37°C for 24 h [35]. MIC was determined based on the broth dilution method using 96 well plates according to NCCLS M27-P (1990).

2.6 Characterization

The formation of Ag/Ag_2O and the reduction reaction of 4-NP and MB were monitored using UV–Visible spectrophotometer (UV-1800, Shimadzu, Japan). The Ag-O vibration bands in Ag/Ag_2O were identified using Fourier transform Infrared spectroscopy (FT-IR) (Thermo Scientific, Nicolet iS50, United States). The crystal structure and phase of Ag/Ag_2O were analyzed by X-ray diffraction (XRD, Rigaku, Miniflex-600, Japan) using Cu Kα radiation (λ = 0.1542 nm). The surface morphology, distribution, and size of Ag/Ag_2O were studied by field emission scanning electron microscope (FESEM) (JEOL, JSM-7100F, Japan), and the element composition was obtained by energy dispersive X-ray (EDX).

3. Results and Discussion

3.1 Characterization of Ag/Ag_2O NPs

3.1.1 UV-Visible and FT-IR spectra

The formation of Ag/Ag_2O NPs was monitored by UV–Visible spectrophotometer. When the Ageratum conyzoides leaves extract was added dropwise into the solution of $AgNO_3$ in the ultrasonic bath at room temperature, the initial colorless solution changed to reddish-brown after 3 min of dropwise addition of plant extract. This reddish-brown color arises due to the excitation of Surface Plasmon Resonance (SPR) vibration in the silver nanoparticles [36]. The color change is owing to the reduction of $Ag^{+} \rightarrow$ Ag by the phytochemicals present in the plant extract, the corresponding SPR peak was observed at λ_{max}= 445 nm (**Fig. 1a**). Similarly, Maham et al., [21] and Ravichandran et al., [37] have reported the SPR peak at λ_{max} 455 nm and 435 nm, respectively. However, Vijayan et al., [19] observed the SPR peak of Ag NPs at 441 nm. The SPR peak indicates the size and morphology of the nanoparticles, and thus, it varies from method to method [19].

The FT-IR spectrum here (**Fig. 1b**) also confirms the presence of Ag_2O. The band at 540 cm^{-1} was assigned to the Ag-O vibration. Similarly, Hosseinpour-Mashkani et al., [38] have reported the Ag-O vibration band at 524 cm^{-1}. However, the bands at 1640 cm^{-1} and 3450 cm^{-1} correspond to the stretching and bending vibration of the O–H bonds of water, respectively. These peaks were observed due to the interaction of physisorbed water molecules with Ag/Ag_2O NPs [39, 40].

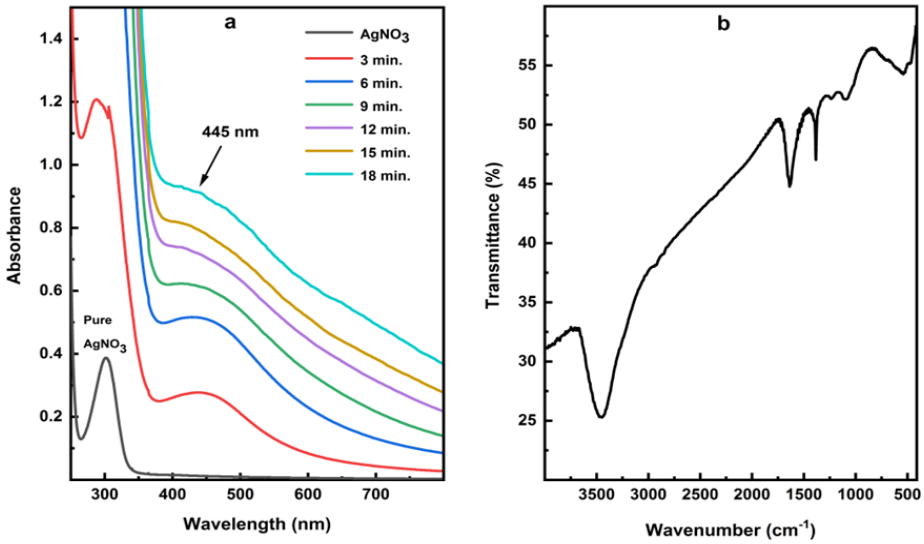

Fig. 1. a) UV-Vis spectra of reaction mixture showing surface plasmon resonance peaks for Ag/Ag_2O nanoparticles (reaction conditions: 2.1 g of $AgNO_3$ in 250 mL distilled water (0.05 M) and 50 mL plant extract in an ultrasonic bath at room temperature). b) FT-IR spectrum of Ag/Ag_2O NPs.

3.1.2 XRD and FESEM-EDX analysis

Fig. 2 shows the diffraction pattern of Ag/Ag_2O NPs, which very well matches with earlier reports for cubic Ag (JCPDS No. 04-0783) [23,41] and Ag_2O (JCPDS No. 00-076-1393) [37]. The diffraction peaks at 2θ = 44.3°, 64.6°, and 77.5° correspond to (200), (200), and (311) planes of metallic Ag. However, the diffraction peaks at 2θ = 27.7°, 32.2°, 38.1°, 46.2°, 54.9°, 57.5°, 67.4°, and 77.3° are indexed to (100), (110), (111), (200), (211), (211), (220), and (311) planes of Ag_2O. Based on Rietveld refinement (not shown here), the fraction of Ag and Ag_2O is close to 50% each. It is presumed that Ag formed initially was oxidized to Ag_2O, leading to a core (Ag) – shell (Ag_2O) structure. Elyamny et al., [42] have reported the one-pot synthesis of Ag @ Ag_2O core-shell nanostructures.

The average crystallite size of the catalyst was estimated using Scherrer's equation 1:

$$D = \frac{0.9\lambda}{dCos\theta} \quad (1)$$

Where d represents the average crystalline size, 0.9 is the crystallite shape constant, λ the wavelength of the X-ray (0.154 nm), β means the full width at half maximum of the peak in radians, and θ is the Bragg's angle of diffraction [43]. Moreover, the Williamson and Hall (W−H) plot was used to estimate the strain using equation 2.

$$\beta \cos\theta = k\lambda/D + 4\varepsilon \sin\theta \quad (2)$$

Where kλ/D is the intercept and ε is the microstrain in the sample. Here, 4 sin θ on the x-axis were plotted against β cos θ on the y-axis to obtain strain from the slope of the line and grain size (D) from the intercept. The crystallite size of the catalyst using Scherrer's equation (1) was found to be ~25 nm. **Fig. S1** shows the W−H plot of the catalyst, which was used to calculate the grain size and strain and it was ~ 5 nm and -0.0067, respectively. A similar observation was reported by Meva et al., [44] and Hatami et al., [45] with Ag and Ag–TiO_2, respectively.

Fig. 3 depicts the FESEM-EDX images of Ag/Ag_2O NPs, which assess the morphology of as-synthesized NPs. FESEM images display the Ag/Ag_2O NPs are irregular in shape. The FESEM images of Ag/Ag_2O NPs (**Fig. 3**) tend to form agglomeration, increasing the particle sizes. A similar, observation was reported by Nezamzadeh-Ejhieh and Karimi-Shamsabadi [46] with CuO-incorporated nano zeolite-X. Therefore, it is difficult to calculate the particle size of nanoparticles using the FESEM images [46]. Further, the EDX data shows around 96 wt.% of the product contains Ag, and the remaining 4 wt.% is O. This corroborates the obtained product is pure Ag/Ag_2O, without any other impurities.

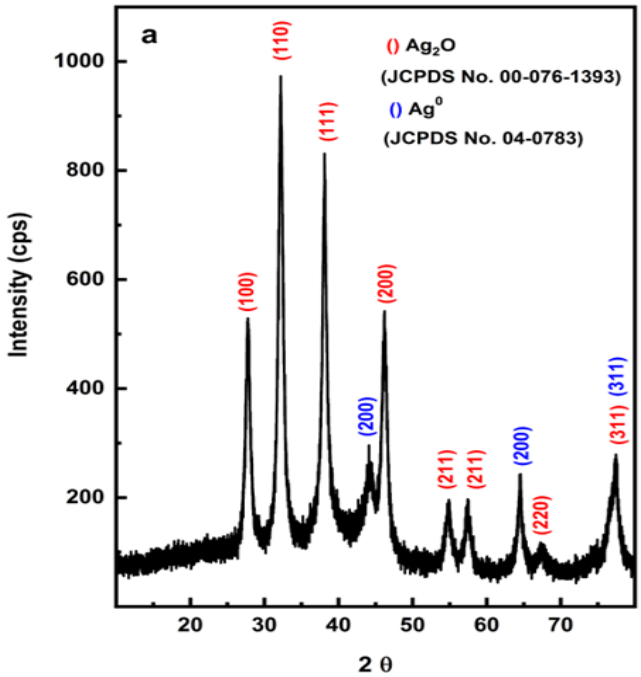

Fig. 2. PXRD pattern Ag/Ag_2O NPs.

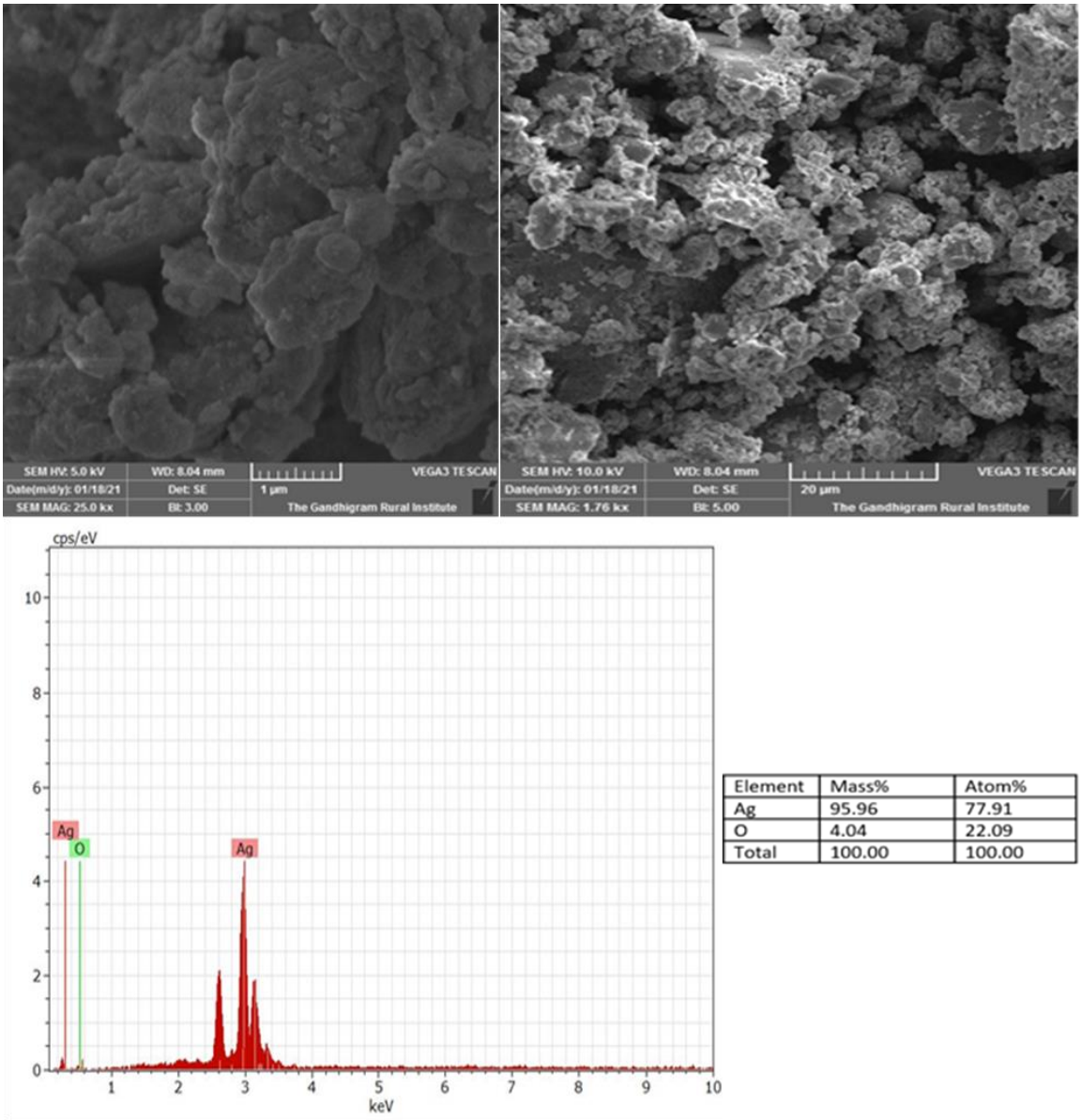

Fig. 3. SEM-EDX images of Ag/Ag_2O NPs.

3.2 Reduction of 4-nitrophenol

The catalytic performance of Ag/Ag_2O NPs was evaluated against 4-NP reduction in the presence of $NaBH_4$ at RT using a UV–Vis spectrophotometer. **Fig. 4a** shows the UV-Vis absorbance spectra of 4-NP alone and 4-NP with $NaBH_4$ solutions. The absorption peaks at 317 nm and 227 nm correspond to the aqueous solution of 4-NP, which appeared due to n → π* and π → π* transitions [19]. A 4-NP solution is light yellow in color and it changes to greenish yellow upon adding $NaBH_4$. This color change was due to an increase in the alkaline nature of the solution mixture. The change in color shifts the position of the absorption peak from 317 nm to 400 nm forming a 4-nitrophenolate ion [8, 19, 32, 47].

The UV-Vis absorption spectra of 4-NP reduction using Ag/Ag_2O NPs in the presence of $NaBH_4$ in an aqueous medium were shown in **Fig. 4b**. Upon $NaBH_4$ addition to the 4-NP solution, results in no reduction of 4-NP. In contrast, the addition of Ag/Ag_2O NPs decreases the intensity at λ_{max} 400 nm. At the same time, a new absorption peak at 298 nm emerged, which corresponds to 4-AP. The reaction of the above reduction process may be written as shown in **Scheme 1**. Deshmukh et al. [8] and Ai et al. [48] reported a similar observation with Ag/TiO_2 and Ag@AMH. To facilitate the 4-NP reduction reaction with $NaBH_4$ in the presence of Ag/Ag_2O NPs. Firstly, both 4-NP and $NaBH_4$ were

adsorbed on the surface of Ag/Ag_2O NPs, where the electron transfer takes place. This is the redox reaction, where 4-NP accepts electron and $NaBH_4$ donate it [19].

To study the effect of $NaBH_4$ volume on 4-NP reduction, experiments were performed by varying $NaBH_4$ (50 mM) volume from 100 µL to 300 µL using 2 mL of 4-NP (0.15 mM) and 1 mg of Ag/Ag_2O NPs (**Fig. 4c**). It was observed that as the volume of $NaBH_4$ increases from 100 µL to 300 µL, the percentage of 4-NP to 4-AP conversion also increases with a marginal difference from 93% to 96%, respectively, in about 10 min. Although, in the case of 300 µL $NaBH_4$, initially, 76% of conversion was achieved within 4 min, however, it was slower down hereafter. Deshmukh et al. [8] and Ai et al. [48] have observed the complete conversion of 4-NP to 4-AP using Ag/ TiO_2 and Ag@ AMH in about 3 and 13 min, respectively.

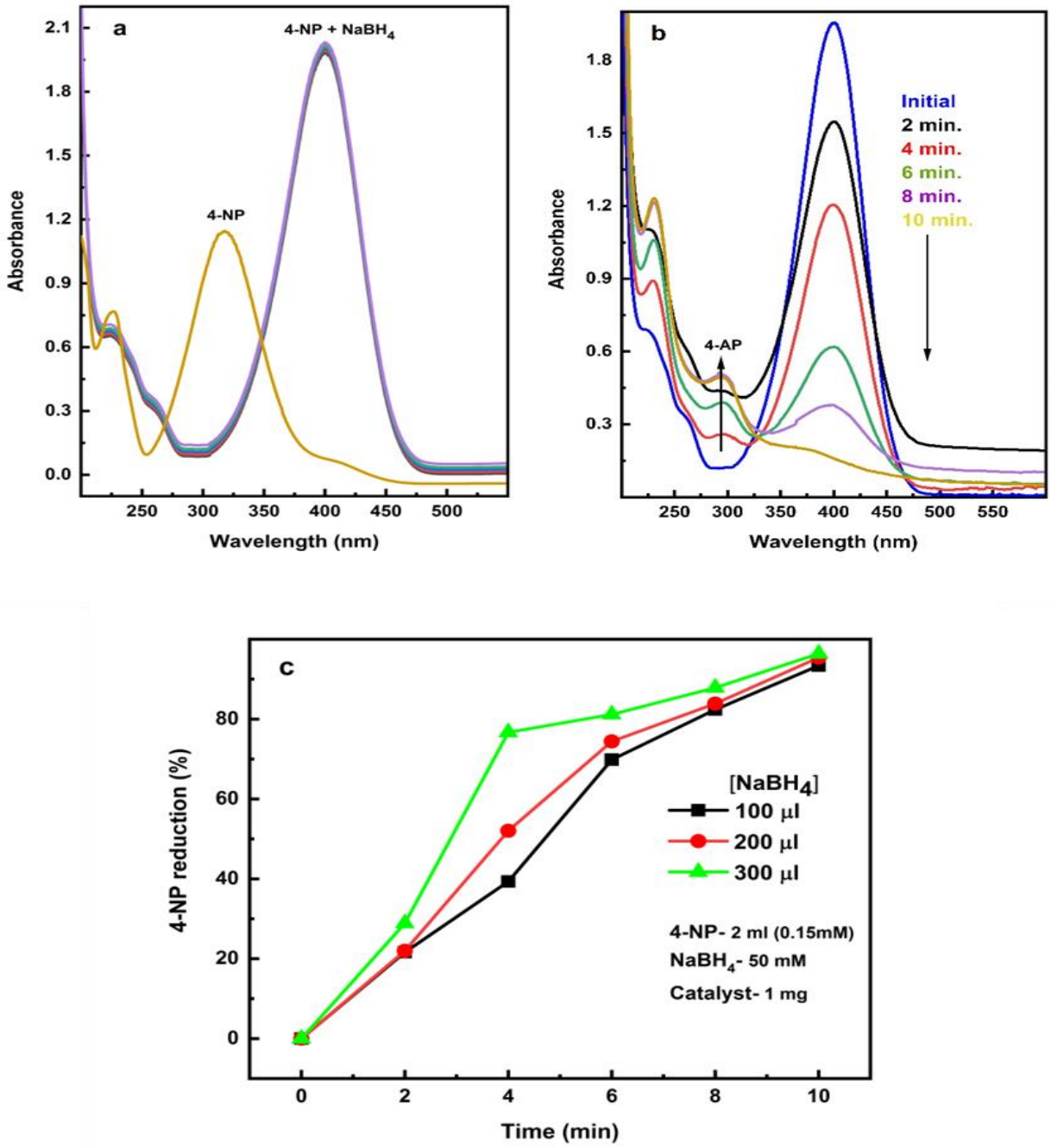

Fig. 4. a) UV-Vis spectra of solutions, 4-NP and 4-NP in $NaBH_4$ without Ag/Ag_2O NPs (reaction conditions: 4-NP= 2 mL (0.15 mM), $NaBH_4$= 100 µL (50 mM)), b) Time-dependent UV-Vis spectra of 4-NP reduction in $NaBH_4$ with Ag/Ag_2O NPs in typical case (reaction conditions: 4-NP= 2 mL (0.15 mM), $NaBH_4$= 100 µL (50 mM), catalyst=1 mg), c) Effect of volume of $NaBH_4$ on the reduction of 4-NP in Ag/Ag_2O NPs using $NaBH_4$.

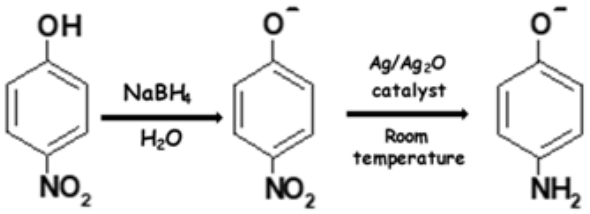

Scheme 1. Catalytic reduction of 4-NP to 4-AP using Ag/Ag_2O NPs.

3.3 Reduction of methylene blue

The catalytic activity of Ag/Ag_2O NPs has been assessed against MB reduction by $NaBH_4$ at room temperature using a UV–Vis spectrophotometer. **Fig. 5a** shows the UV-Vis spectra of MB reduction using Ag/Ag_2O NPs in the presence of $NaBH_4$ in a typical case. Here, the absorption band for MB was obtained at 665 nm and 290 nm due to the transition of n → π* and π → π* [19]. The additions of $NaBH_4$ into the solution of MB dye do not alter the intensity of the absorption peak at 665 nm. From these observations, it was corroborated that $NaBH_4$ alone does not reduce MB. This was owing to the high reduction potential difference between MB and $NaBH_4$. This reaction is thermally allowed but kinetically forbidden [19]. However, upon the addition of Ag/Ag_2O NPs to the solution of MB and $NaBH_4$ gradual decrease in the intensity at 665 nm was observed (**Scheme 2**), which directly reflects the reduction of MB dye and complete reduction takes place in about 6 min (**Fig. 5a**). Bhosale et al., [39] and Zheng et al., [49] reported a similar observation with Cu_2O and Ag in the presence of $NaBH_4$. As the reduction of MB takes place, the intensity at 665 nm decreases, concurrently a new peak at 256 nm emerges, and its intensity increases with time owing to the formation of leuco MB [19].

The effect of $NaBH_4$, its concentration, and the catalyst was studied using 2 mL MB (10 ppm) solution, and the progress in the reduction reaction was observed by UV–Vis spectrophotometer. The mixture of MB and 100 µL of $NaBH_4$ (30 mM) without Ag/Ag_2O NPs show a negligible (13%) reduction of MB dye (**Fig. 5b**). However, MB in the presence of 1 mg Ag/Ag_2O NPs without $NaBH_4$ shows 17% of the decrease in intensity at 665 nm in about 6 min, which corresponds to the adsorption of dye on the catalyst. Furthermore, the MB reduction (2 mL, 10 ppm) was carried out at 100 µL and 200 µL $NaBH_4$ (30 mM) using 1 mg, Ag/Ag_2O NPs. In the case of 100 µL of $NaBH_4$, about 94% reduction took place in 6 min, whereas it was about 97% in the case of 200 µL $NaBH_4$ in 3 min (**Fig. 5b**).

3.4 Antibacterial activity

Invitro antibacterial activity of the Ag/Ag_2O NPs was tested against the different bacteria S. mutans, B. subtilis, and E. coli bacteria. The Ag/Ag_2O NPs show good antibacterial activity against S. mutans and E. coli bacteria. **Fig 6** shows the MIC against three different bacteria. The MIC against S. mutans and E. coli is found to be 2.5 mg/mL and less than 0.0781 mg/mL, respectively. The diameter (cm) of the zone of inhibition was represented in **Fig. S2** and also tabulated in **Table 1**. Using 10 mg/mL of Ag/Ag_2O NPs against S. mutans, B. subtilis, and E. coli bacteria the diameter of the zone of inhibition are 1.9 cm, 0.6 cm, and 2.4 cm. Here, the Ag/Ag_2O NPs show good antibacterial activity against E. coli.

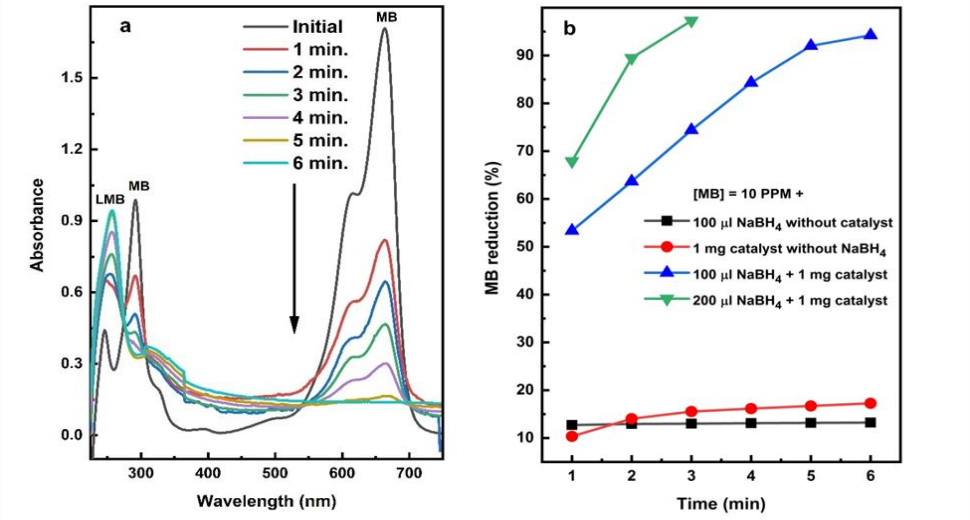

Fig. 5. a) Time-dependent UV-Vis spectra of MB reduction in $NaBH_4$ with Ag/Ag_2O NPs in typical case (reaction conditions: MB = 2 mL (10 ppm), $NaBH_4$= 100 µL (30 mM), catalyst=1 mg), (b) Kinetic study of MB reduction using 10 ppm MB solution.

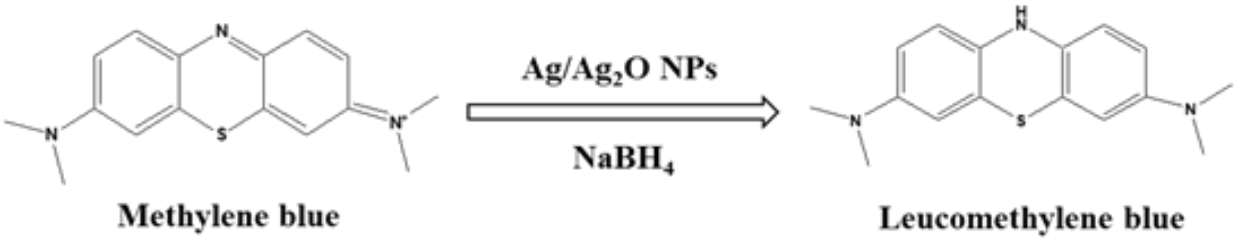

Scheme 2. Catalytic reduction of MB to LMB using Ag/Ag_2O NPs.

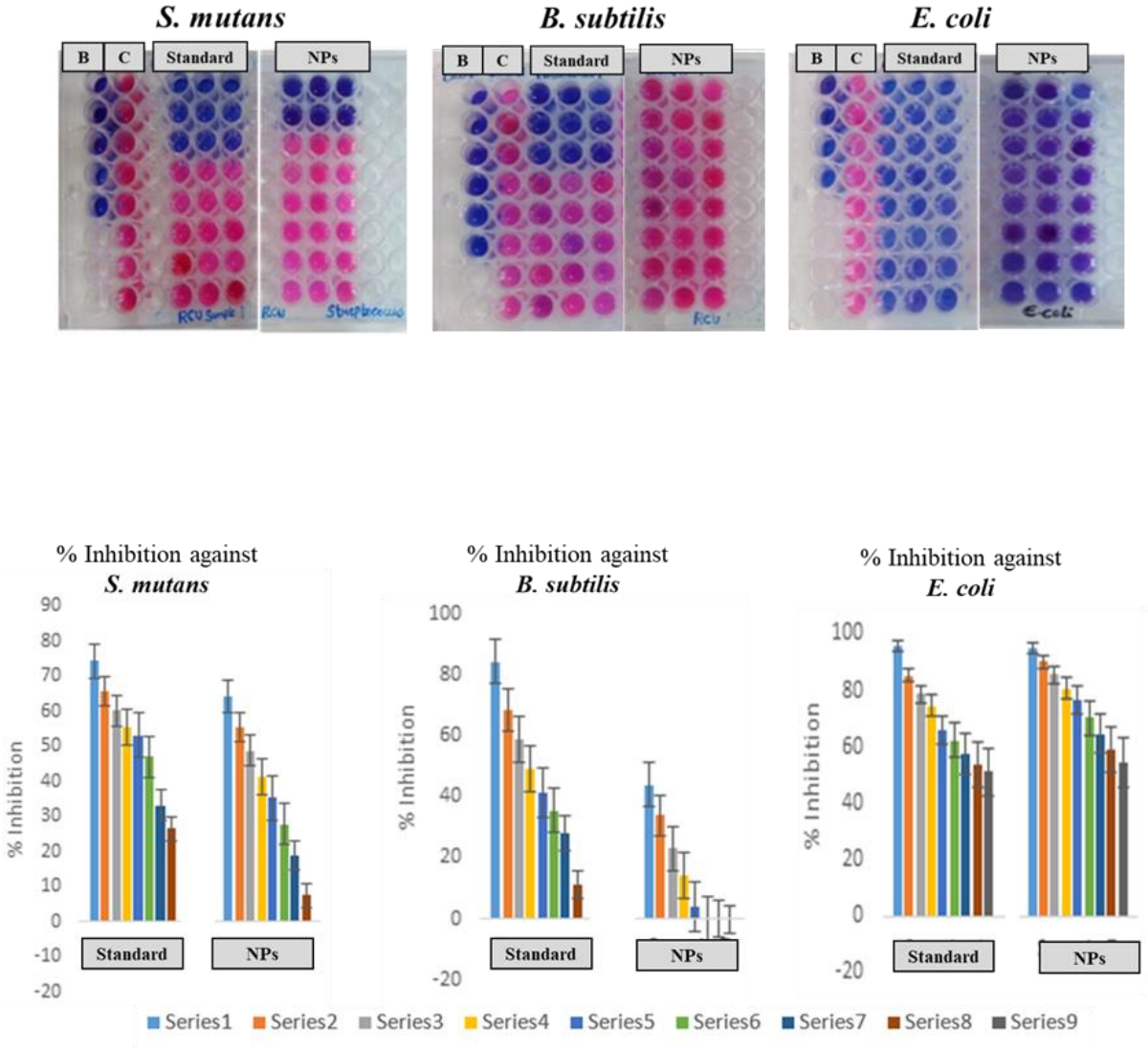

Fig. 6. MIC against different bacteria *S. mutans*, *B. subtilis* and *E. coli*.

Table 1. Antibacterial activity of Ag/Ag_2O NPs against bacterial pathogens.

Ag/Ag_2O nanoparticles	*S. mutans*	*B. subtilis*	*E. coli*
Standard (Streptomycin)	2.1 cm	1 cm	2.1 cm
5 mg/mL	1.8 cm	0.6 cm	NS
10 mg/mL	1.9 cm	0.6 cm	2.4 cm

NS: Not studied

4. Conclusions

Here, ultrasound synthesis of Ag/Ag_2O NPs was reported using aqueous leaf extract of Ageratum conyzoides agriculture weed. The obtained NPs were stable and exhibited excellent catalytic activity towards the reduction of organic pollutants such as 4-NP and MB dye in the presence of $NaBH_4$. Furthermore, Ag/Ag_2O NPs have been tested for their bactericidal activity against Streptococcus mutans, B. subtilis, and E. coli bacteria. This study successfully utilizes the agricultural weed to synthesize Ag/Ag_2O NPs by a simple reduction process. Therefore, we believe that the present method is simple and environmentally benign towards synthesizing catalysts and its application in wastewater treatment.

Acknowledgements

The principal author Mr. Dinesh Patil thankful to Rani Channamma University, Belagavi, Karnataka, India for funding support and research facility.

References

[1] K.B. Narayanan, N. Sakthivel, Bioresour. Technol. 102 (2011) 10737-10740.

[2] P.K. Arora, A. Srivastava, V.P.Singh, J. Hazard. Mater. 266 (2014) 42-59.

[3] Z. Xiong, H. Zhang, W. Zhang, B. Lai, G. Yao, Chem. Eng. J. 359 (2019) 13-31.

[4] Y. Yuan, B. Lai, Y.Y. Tang, Chem. Eng. J. 283 (2016) 1514-1521.

[5] Z.I. Bhatti, H. Toda, K. Furukawa, Water Res. 36 (2002) 1135-1142.

[6] N. Pradhan, A. Pal, T. Pal, Colloids Surf. 196 (2002) 247–257.

[7] S.K. Ghosh, M. Mandal, S. Kundu, S. Nath, T. Pal, Appl. Catal. A Gen. 268 (2004) 61–66.

[8] S.P. Deshmukh, R.K. Dhokale, H.M. Yadav, S.N. Achary, S.D. Delekar, Appl. Surf. Sci. 273 (2013) 676-683.

[9] Q. Hu, X. Liu, L. Tang, D. Min, T. Shia, W. Zhang, RSC Adv. 7 (2017) 7964–7972.

[10] X.Y. Dong, Z.W. Gao, K.F. Yang, W.Q. Zhang, L.W. Xu, Catal. Sci. Technol. 5 (2015) 2554–2574.

[11] H. Derikvandi, A. Nezamzadeh-Ejhieh, J. Haz. Mat. 321 (2017) 629–638.

[12] N.E. Farda, R. Fazaelib, Iran. J. Catal. 8(2) (2018) 133–141.

[13] T. Tamiji, A. Nezamzadeh-Ejhieh, J. Ele. Chem. 829 (2018) 95–105.

[14] A. Hiskia, A. Troupis, S. Antonaraki, E. Gkika, P. Kormali, E. Papaconstantinou, Intern. J. Environ. Anal. Chem. 86 (2006) 233–242.

[15] R.N. Bharagava, G. Saxena, S.I. Mulla, in: G. Saxena, R. Bharagava, (Eds.) Bioremediation of Industrial Waste for Environmental Safety, Springer, Singapore, 2020, pp. 1–18.

[16] I. Ahmad, M. Imran, M.B. Hussain, S. Hussain, N.A. Anjum, in: N.A. Anjum. (Eds.) Chemical Pollution Control with Microorganisms, Nova Sci. Publisher, 2017, pp. 197-243.

[17] Textile dyes market., 2022. Textile dyes market by dye type, fiber type, and region-Global forecast to 2027. markets and markets CH6147. https://www.marketsandmarkets.com/Market-Reports/textile-dye-market-226167405.html.

[18] Fibre2Fashion, Booming textile dyes industry in emerging economies (2014). www.fibre2fashion.com

[19] R. Vijayan, S. Joseph, B. Mathew, Bio. Nano. Sci. 8 (2018) 105–117.

[20] S.K. Chandraker, M. Lal, R. Shukla, RSC Adv. 9 (2019) 23408.

[21] M. Maham, M. Nasrollahzadeh, S.M. Sajadi, Compos. B. Eng. 185 (2020) 107783.

[22] W. Jiang, X. Wang, Z. Wu, X. Yue, S. Yuan, H. Lu, B. Liang, Ind. Eng. Chem. Res. 54 (2015) 832−841.

[23] S. Akel, R. Dillert, N.O. Balayeva, R. Boughaled, J. Koch, M.E. Azzouzi, D.W. Bahnemann, Catalysts 8, (2018) 647.

[24] N. Bi, H. Zheng, Y. Zhu, W. Jiang, B. Liang, J. Environ. Chem. Eng. 6(2) (2018) 3150-3160.

[25] E.E. Elemike, D.C. Onwudiwe, A.C. Ekennia, C.U. Sonde, R.C. Ehiri, Molecules 22, (2017) 674.

[26] S. Yallappa, J. Manjanna, B.L. Dhananjaya, Spectrochim. Acta A 137 (2015) 236-243.

[27] X. Wang, S. Li, H. Yu, J. Yu, S. Liu, Chem. Eur. J. 17 (2011) 7777−7780.

[28] A. Kadam, R. Dhabbe, A. Gophane, T. Sathe, K. Garadkar, J. Photochem. Photobiol. B 154 (2016) 24−33.

[29] M. Xu, L. Han, S. Dong, ACS Appl. Mater. Interfaces 5 (2013) 12533−12540.

[30] A.L. Okunade, Fitoterapia 73 (2002) 1-16.

[31] V.H. Thorat, S.S. Ghorpade, T. Patole, Int. J. Pharmacogn. 5(4) (2018) 213-218.

[32] D. Patil, J. Manjanna, S. Chikkamath, V. Upper, M. Chougala, J. Hazard. Mater. Adv. 4 (2021) 100032

[33] M. Sultan, A. Javeed, M. Uroos, M. Imran, F. Jubeen, S. Nouren, N. Saleem, I. Bibi, R. Masood, W. Ahmed, J. Hazard. Mater. 344 (2018) 210–219.

[34] A. Raza, M. Ikram, M. Aqeel, M. Imran, A. Ul-Hamid, K.N. Riaz,·S. Ali, Appl. Nanosci. 10 (2020) 535–1544.

[35] Z.H.A. El-Wahab, M.M. Mashaly, A.A. Salman, B.A. El-Shetary, A.A. Faheim, Spectrochim. Acta A 60 (12) (2004) 2861–2873.

[36] J. Saha, A. Begum, A. Mukherjee, S. Kumar, Sustain. Environ. Res. 27(5) (2017) 245-250.

[37] S. Ravichandran, V. Paluri, G. Kumar, K. Loganathan, B.R.K. Venkata, J. Exp. Nanosci. 11(6) (2016) 445–458.

[38] S.M. Hosseinpour-Mashkani, R. Majid, Mater. Lett. 130 (2014) 259–262.

[39] M.A. Bhosale, S.C. Karekar, B.M. Bhanage, Chemistry Select 1 (2016) 6297-6307.

[40] I. Roy, A. Bhattacharyya, G. Sarkar, N.R. Saha, D. Rana, P.P. Ghosh, M. Palit, A.R. Das, D. Chattopadhyay, RSC Adv. 4 (2014) 52044-52052.

[41] L. Zhou, G. Zou, H. Deng, Catalysts 8 (2018) 272.

[42] S. Elyamny, M. Eltarahony, M. Abu-serie, M. Nabil, A. Kashyout, Sci. Rep. 11 (2021) 22543.

[43] A. Nezamzadeh-Ejhieh, M. Karimi-Shamsabadi, Appl. Catal. A Gen. 477 (2014) 83–92.

[44] F. Meva, J. Mbeng, C. Ebongue, C. Schlüsener, U. Kökçam-Demir, A. Ntoumba, P. Kedi, E. Elanga, E. Loudang, M. Nko'o, E. Tchoumbi, V. Deli, C. Nanga, E. Mpondo, C. Janiak, J. Bio. Nanobio. 10 (2019) 102–119.

[45] M. Hatami, K.V. Rao, M. Ahmadipour, V. Rajendar, Adv. Sci. Eng. Med. 5 (2013) 1–5.

[46] A. Nezamzadeh-Ejhieh, M. Karimi-Shamsabadi, Chem. Eng. J. 228 (2013) 631–641.

[47] X. Yang, H. Zhong, Y. Zhu, H. Jiang, J. Shen, J. Huang, C. Li, J. Mater. Chem. A 2 (2014) 9040-9047.

[48] L. Ai, H. Yue, J. Jiang, J. Mater. Chem. 22 (2012) 23447-23453.

[49] Y. Zheng, A. Wang, J. Mater. Chem. 22 (2012) 16552–16559.